Compensation of Frequency–Selective I/Q Imbalances in Wideband Receivers: Models and Algorithms

Mikko Valkama and Markku Renfors
Telecommunications Laboratory
Tampere University of Technology
P.O. Box 553, FIN-33101 Tampere, Finland
E-mail: {valkama,mr}@cs.tut.fi

Visa Koivunen
Signal Processing Laboratory
Helsinki University of Technology
P.O. Box 3000, FIN-02015 HUT, Finland
E-mail: visa.koivunen@hut.fi

Abstract – **To achieve satisfactory performance in analog I/Q (inphase/quadrature) processing based wireless receivers, the matching of amplitudes and phases of the I and Q branches becomes vital. In practice, there is always some imbalance and the image attenuation produced by the analog processing remains finite. Especially in wideband receivers, where the existence of strong image band signals makes the attenuation requirements extremely stringent, analog processing is incapable of providing adequate image rejection. In this paper, we derive a general frequency-dependent signal model for an imbalanced analog front-end and present two alternative methods utilizing digital processing to enhance the analog front-end image rejection. Based on the obtained results, the proposed methods provide adequate image signal rejection with very few assumptions, even in the difficult cases of frequency-selective and/or time-varying imbalances.**

I. Introduction

Due to the inherent two-path structure, analog I/Q signal processing is in general extremely sensitive to mismatches between the I and Q branches [1]-[9]. With practical analog electronics, imbalances are unavoidable which result in imperfect image rejection. Whether the finite image rejection of the analog processing is sufficient or not, depends on the applied architecture [1]-[5], [9].

In wideband receivers, a multichannel signal (in the extreme case the whole service band) is digitized as a whole and the final channel selection and demodulation are done using digital signal processing (DSP) in a flexible way [9]. Then, since the image frequency band may carry a signal at the maximum allowed blocking signal level, the basic I/Q downconversion approaches cannot be used in the wideband case due to the imbalance problem. Digital compensation techniques could be a way to get around this limitation, and make simple analog front-ends feasible also in wideband receivers.

Both analog and digital techniques to compensate for the effects of mismatches are available in the literature, see, e.g., [1]-[8]. In this paper, novel digital methods for obtaining adequate image attenuation are presented. In contrast to many existing approaches, the proposed methods can provide sufficient compensation performance even when the imbalances are frequency-selective and/or time-varying. Furthermore, no training signals or prior knowledge of the front-end imbalances are needed.

The paper is organized as follows. In Section II, a general signal model for an imbalanced analog front-end is derived. In Section III, two alternative imbalance compensation methods are presented utilizing traditional adaptive interference cancellation (IC) or more recent multichannel blind deconvolution (MBD) techniques. Simulation results are presented in Section IV and conclusion are drawn in Section V.

II. General Imbalance Model

A. Front-End Model

A generalized block-diagram of an analog I/Q signal processing based quadrature receiver [2], [10] is presented in Fig. 1. In general, all the analog components, such as quadrature demodulator, branch filters, and A/D converters, affecting the I and Q branch signals contribute to the effective amplitude and phase mismatches [1], [2], [5], [8]. Thus, to formally analyze the mismatch effects, a simplified model for an imbalanced analog front-end is introduced in Fig. 2.

The effect of quadrature demodulator: The local oscillator signal $x_{LO}(t)$ of an imbalanced quadrature demodulator is here modelled as

$$\begin{aligned} x_{LO}(t) &= \cos(2\pi f_C t) - jg\sin(2\pi f_C t + \phi) \\ &= K_1 e^{-j2\pi f_C t} + K_2 e^{j2\pi f_C t}, \end{aligned} \tag{1}$$

where g and ϕ represent the demodulator amplitude and phase imbalances, respectively (ideally $g = 1$ and $\phi = 0$). The mismatch coefficients K_1 and K_2 in (1) are given by

$$K_1 = [1 + ge^{-j\phi}]/2, \tag{2a}$$

$$K_2 = [1 - ge^{j\phi}]/2. \tag{2b}$$

The effect of branch components: The branch component mismatches can be easily modeled as imbalanced lowpass filters (LPF) as given by

$$H_{LPF,I}(f) = H_{NOM}(f)H_I(f), \tag{3a}$$

$$H_{LPF,Q}(f) = H_{NOM}(f)H_Q(f), \tag{3b}$$

where $H_{NOM}(f)$ is the nominal LPF response. $H_I(f)$ and $H_Q(f)$ represent the actual mismatch effects, i.e., with perfect matching, $H_I(f) = H_Q(f)$.

B. Wideband Signal Model

To explicitly characterize the imbalance effects on the individual channel signals, we write the multichannel received signal $r(t)$ (centered at f_C with a bandwidth B) formally as [10]

$$r(t) = 2\,\mathrm{Re}[z(t)e^{j2\pi f_C t}] = z(t)e^{j2\pi f_C t} + z^*(t)e^{-j2\pi f_C t}, \tag{4}$$

where * denotes complex conjugation and $z(t) = z_I(t) + jz_Q(t)$ is the baseband equivalent signal of $r(t)$. As a model (Fig. 2), the received signal $r(t)$ is downconverted to baseband by mixing it with $x_{LO}(t)$ of (1). Assuming that $H_{NOM}(f) = 1$ for $|f| \le B/2$ and $H_{NOM}(f) = 0$ for $|f| > B/2$, the downconverted signal $x(t)$ can be easily written as

$$x(t) = K_1 z(t) + K_2 z^*(t). \tag{5}$$

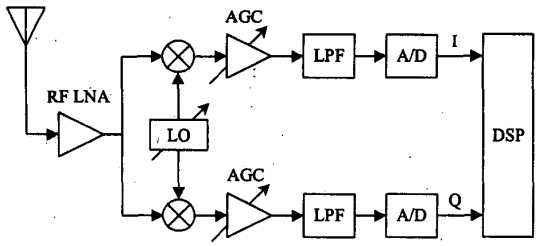

Fig. 1. Generalized model for I/Q processing based quadrature receiver. The I and Q branch signals are generated using analog processing.

To analyze the effect of branch mismatches, the signal of (5) can first be written as $x(t) = x_I(t) + jx_Q(t)$, where

$$x_I(t) = z_I(t), \tag{6a}$$

$$x_Q(t) = g\cos(\phi)z_Q(t) - g\sin(\phi)z_I(t). \tag{6b}$$

Then, in terms of Fourier transforms, the signal $z'(t) = z_I'(t) + jz_Q'(t)$ after branch mismatches is given by

$$\begin{aligned} Z'(f) &= Z_I'(f) + jZ_Q'(f) \\ &= X_I(f)H_I(f) + jX_Q(f)H_Q(f) \\ &= Z_I(f)[H_I(f) - jH_Q(f)g\sin(\phi)] \\ &\quad + jZ_Q(f)[H_Q(f)g\cos(\phi)]. \end{aligned} \tag{7}$$

After some manipulations, the result of (7) can be written in a more convenient form as

$$Z'(f) = G_1(f)Z(f) + G_2(f)Z^*(-f), \tag{8}$$

where

$$G_1(f) = [H_I(f) + H_Q(f)ge^{-j\phi}]/2, \tag{9a}$$

$$G_2(f) = [H_I(f) - H_Q(f)ge^{j\phi}]/2. \tag{9b}$$

In (8), the term relative to $Z^*(-f)$ is caused by the imbalances and represents the image aliasing effect. Then, the image attenuation of the analog front-end processing can be defined as

$$L(f) = |G_1(f)|^2 / |G_2(f)|^2. \tag{10}$$

With practical analog electronics, this attenuation is usually in the order of 20...40 dB. Notice that the basic imbalance model used in [3]-[5] is a special case of (8) for which $H_I(f) = H_Q(f)$. The basic imbalance effect is further illustrated for wideband multichannel downconversion in Fig. 3. The desired signal is depicted in grey and the interfering image signal in dark. Clearly, the front-end processing cannot sufficiently attenuate the image band signal and some kind of compensation is needed.

III. Digital Imbalance Compensation

Here, in our formulation, the task of imbalance compensation is to enhance the finite image attenuation $L(f)$ of the analog processing. More precisely, the target is to obtain an image-free observation of a specific channel (referred to as the desired channel) signal located at non-zero intermediate frequency (IF) after the initial wideband downconversion.

A. Two Baseband Observations

As in the ideal (perfect matching) case, the multichannel signal $Z'(f)$ contains a desired signal component and an image component around $+f_{IF}$ and $-f_{IF}$, respectively. Due to imbalances (see (8) and Fig. 3), $Z'(f)$ has a disturbing image signal component around $+f_{IF}$ but also a desired signal component around $-f_{IF}$. Motivated by this, we generate *two* observations, $d(t)$ and $v(t)$, where $d(t)$ is the baseband observation of the combined signal around $+f_{IF}$ and $v(t)$ is the mirrored (complex-conjugated) baseband observation of the combined signal around $-f_{IF}$ [3]-[5]. After some manipulations, the frequency domain expression for these observations can be written in matrix formulation as

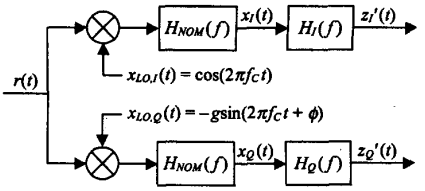

Fig. 2. Imbalance model for the analog front-end including the effects of both the quadrature demodulator and the branch components.

$$\mathbf{X}(f) = \mathbf{A}(f)\mathbf{S}(f), \tag{11}$$

where $\mathbf{X}(f) = [D(f)\ V(f)]^T$, $\mathbf{S}(f) = [S(f)\ I^*(-f)]^T$, and $s(t)$ and $i(t)$ denote the baseband equivalents of the desired and image signals, respectively. The matrix $\mathbf{A}(f)$ is given by

$$\mathbf{A}(f) = \begin{bmatrix} G_1(f+f_{IF}) & G_2(f+f_{IF}) \\ G_2^*(-f-f_{IF}) & G_1^*(-f-f_{IF}) \end{bmatrix} \Pi(f, B_C), \tag{12}$$

where B_C denotes the individual channel bandwidth and $\Pi(f, B_C) = 1$ for $|f| \le B_C/2$ and zero otherwise. Even though the baseband model (11) was here derived in continuous-time domain, the observations can in practice be generated digitally, thus avoiding any excess imbalance effects [5]. Consequently, discrete-time notations $d(n)$, $v(n)$, $s(n)$, and $i(n)$ are used hereafter, and the observed signals $x_1(n) = d(n)$ and $x_2(n) = v(n)$ appear as convolutive mixtures of the effective source sequences $s_1(n) = s(n)$ and $s_2(n) = i^*(n)$.

B. Adaptive Interference Cancellation (IC)

If the desired channel signal is originally more powerful than the image signal, the image attenuation of analog processing is sufficient, and thus, the desired channel observation $d(n)$ can be used directly as an estimate of $s(n)$. On the other hand, in the difficult case of a strong image signal, when the attenuation of (10) is insufficient, $v(n)$ is highly correlated with the interfering signal component but only weakly correlated with the desired signal component of $d(n)$ [3], [5], [11]. Motivated by this, adaptive interference canceller [11] can be used to estimate $s(n)$ as

$$\hat{s}_{IC}(n) = d(n) - \sum_{k=0}^{N_{IC}} w_k(n)v(n-k), \tag{13}$$

where the filter coefficients $w_k(n)$, $k = \{0, \ldots, N_{IC}\}$, can be adapted with any available algorithm, such as the least-mean-square (LMS) or recursive least-squares (RLS) algorithms [11].

C. Multichannel Blind Deconvolution (MBD)

Based on the observed mixtures of statistically independent source signals, the task of multichannel blind deconvolution is in general to recover the original source contributions, without knowing the actual mixture parameters [12], [13]. Assuming that the different channel signals are independent, the signal model of

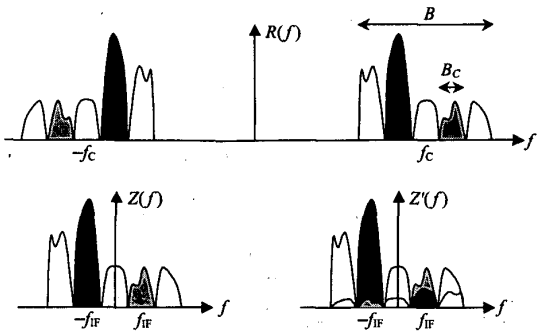

Fig. 3. The received signal $R(f)$ and the ideal and imbalanced baseband equivalent signals $Z(f)$ and $Z'(f)$. The desired channel signal (grey) is heavily interfered by the image signal (dark).

(11) fits directly to this formulation [5]. With reasonable analog design, the matrix $\mathbf{A}(f)$ of (12) is invertible, and a multichannel blind deconvolution algorithm, such as the one proposed in [13], can indeed be used to estimate the desired signal $s(n)$ as well as the interfering signal $i(n)$. More formally, the estimate of the source vector $\mathbf{s}(n) = [s(n)\ i^*(n)]^T$ is given (up to permutation and scaling) by

$$\hat{\mathbf{s}}(n) = \sum_{k=0}^{N_{MBD}} \mathbf{W}_k(n)\mathbf{x}(n-k), \qquad (14a)$$

where $\mathbf{x}(n) = [d(n)\ v(n)]^T$, and the actual desired channel signal $s(n)$ is estimated as

$$\hat{s}_{MBD}(n) = \mathbf{e}_i^T \hat{\mathbf{s}}(n),\ i = 1 \text{ or } 2, \qquad (14b)$$

where $\mathbf{e}_1 = [1\ 0]^T$ or $\mathbf{e}_2 = [0\ 1]^T$ is used, depending on the possible source permutation. In general, there exists a wide variety of different approaches (see [12] for an excellent review) to measure the independence of the separated output signals, and thus, to adapt the demixing matrices $\mathbf{W}_k(n)$, $k = \{0, \ldots, N_{MBD}\}$.

IV. Simulations

To illustrate the effectiveness of the proposed compensation methods, example MATLAB simulations are carried out.

Front-End Parameters: The received signal consists of the desired and image channels of bandwidth 0.2π located originally around 0.7π and 0.3π, respectively. The desired and image signals are QPSK- and 8PSK-modulated, respectively, with raised-cosine pulse-shapes (roll-off 0.35). The relative power difference is -30 dB. In translating the desired channel signal to an IF of 0.2π, imbalance values of $g = 1.02$ and $\phi = -2°$ are used for the quadrature demodulator. After that, the branch mismatches are modeled as $H_I(z) = 0.01 + z^{-1} + 0.01z^{-2}$ and $H_Q(z) = 0.01 + z^{-1} + 0.2z^{-2}$. These front-end imbalance properties are illustrated in Figs. 4 and 5. Finally, the symbol rate baseband observations $d(n)$ and $v(n)$ are generated by proper frequency translations of $\pm 0.2\pi$, lowpass filtering, and decimation.

With the given front-end, the image attenuation is in the order of 20 dB. As a consequence, since the image signal is originally 30 dB more powerful than the desired signal, the interfering signal component of $d(n)$ is of 10 dB higher power level than the desired component itself.

IC Simulation: The standard RLS algorithm [11] with a forgetting factor of 0.9999 (asymptotic sample length of 10 000 samples) is used to adapt the IC filter of length 5 ($N_{IC} = 4$). The total number of samples is 2000 to quarantee a steady-state operation.

MBD Simulation: The natural gradient based algorithm of [13] is used with a step-size of 0.001 to adapt the demixing filters of length 5 ($N_{MBD} = 4$). After initial convergence, the step-size is reduced to 0.0002. The total number of samples is 12 000 to quarantee a steady-state operation. To stabilize the adaptation, the input signals $x_1(n) = d(n)$ and $x_2(n) = v(n)$ of the demixing filters are normalized as

$$x_1(n) \leftarrow x_1(n)/\sqrt{P_1}\ , \qquad (15a)$$

$$x_2(n) \leftarrow x_2(n)/\sqrt{P_2}\ . \qquad (15b)$$

The power estimates $P_1(n)$ and $P_2(n)$ can, e.g., be obtained recursively as

$$P_i(n) = 0.995P_i(n-1) + 0.005\left|x_i(n)\right|^2,\ i = 1 \text{ and } 2. \qquad (15c)$$

Comparisons: Single realizations of the absolute value of $w_2(n)$ and $W_{2,ij}(n) = [\mathbf{W}_2(n)]_{ij}$ are presented in Figs. 6 and 7 to illustrate the convergence properties. Clearly, the IC algorithm converges much faster than the MBD algorithm. However, as verified by Fig. 8, there is no difference in the steady-state operation between the two methods. Furthermore, due to their adaptive nature, both the IC and MBD based methods are able to track the possible time-variations in the analog front-end.

In general, the IC based compensator is only utilizable if the image signal is more powerful than the desired channel signal. Consequently, some kind of power estimation of the different channel signals is needed to decide when to switch the IC structure on and off. This problem, usually referred to as signal leakage, can in theory be avoided using the MBD based compensator, though, as mentioned in Section III, no compensation is actually needed if the image signal is weak. On the other hand, the performance of the IC based solution is likely to be less sensitive to the effects of additive noise and, especially, to different interferer types. For a more detailed discussion on the relative merits of interference cancellation and blind deconvolution (or signal separation) based techniques, see [5].

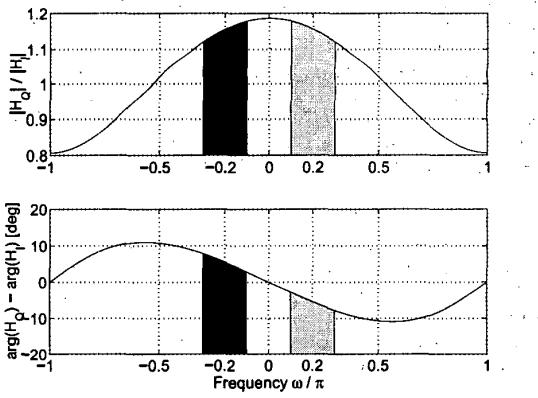

Fig. 4. Relative amplitude and phase mismatches of the branch components. Positive (grey) and negative (dark) IF bands are illustrated in different colours.

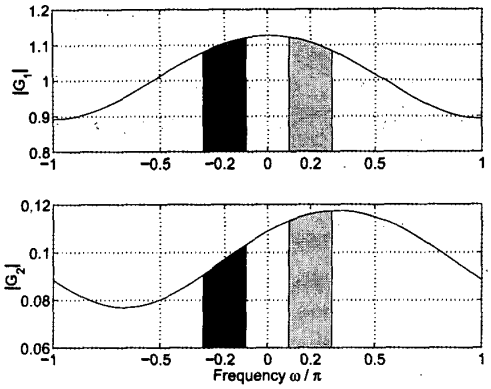

Fig. 5. General imbalance coefficients G_1 and G_2. Positive (grey) and negative (dark) IF bands are illustrated in different colours.

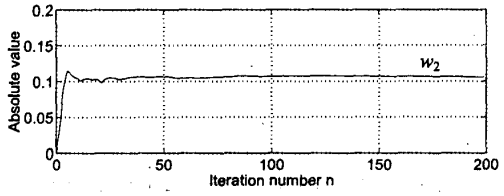

Fig. 6. Center tap value $w_2(n)$ of the RLS based interference canceller, forgetting factor 0.9999.

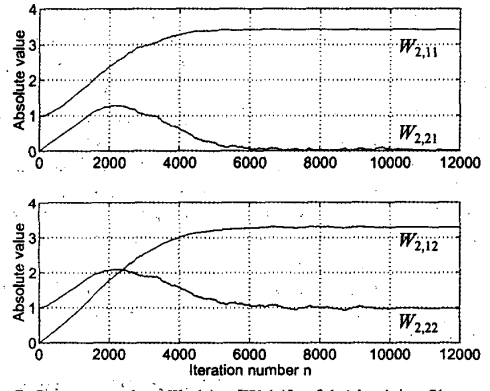

Fig. 7. Center tap values $W_{2,ij}(n) = [\mathbf{W}_2(n)]_{ij}$ of the demixing filters using the natural gradient algorithm, step-size 0.001 (initially) and 0.0002 (after convergence).

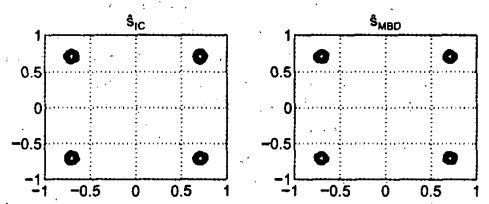

Fig. 8. Compensated output samples after convergence of both the IC (left) and MBD (right) based compensators. Also shown are the ideal QPSK symbol locations (white asterisks).

V. Conclusions

In this paper, we derived a model for I/Q imbalance compensation in wideband receivers. The model is generic in the sense that it covers time-varying and frequency-selective imbalances as well. Two compensation algorithms were proposed. One stems from the well-known adaptive interference cancellation approach whereas the other is based on the multichannel blind separation of convolutive mixtures [13]. The results indicate that the proposed methods can provide adequate image signal rejection even in the difficult cases of frequency-selective and time-varying imbalances. In addition, the methods are robust in a sense that very few, relaxed assumptions are needed in deriving them.

Acknowledgment

This work was supported by the Academy of Finland, the Graduate School in Electronics, Telecommunications and Automation (GETA), and the Nokia Foundation.

References

[1] J. Crols and M. S. J. Steyaert, "Low-IF topologies for high-performance analog front ends of fully integrated receivers," *IEEE Trans. Circuits Syst. II*, vol. 45, pp. 269-282, Mar. 1998.

[2] J. Tsui, *Digital Techniques for Wideband Receivers*. Norwood, MA: Artech House, 1995.

[3] M. Valkama and M. Renfors, "Advanced DSP for I/Q imbalance compensation in a low-IF receiver," in *Proc. IEEE Int. Conf. on Communications*, New Orleans, LA, USA, Jun. 2000, pp. 768-772.

[4] M. Valkama, M. Renfors, and V. Koivunen, "Blind source separation based I/Q imbalance compensation," in *Proc. IEEE Symposium 2000 on Adaptive Systems for Signal Processing, Communications and Control*, Lake Louise, Alberta, Canada, Oct. 2000, pp. 310-314.

[5] M. Valkama, M. Renfors, and V. Koivunen, "Advanced methods for I/Q imbalance compensation in communication receivers," submitted to *IEEE Trans. Signal Processing*.

[6] J. K. Cavers and M. W. Liao, "Adaptive compensation for imbalance and offset losses in direct conversion transceivers," *IEEE Trans. Veh. Technol.*, vol. 42, pp. 581-588, Nov. 1993.

[7] J. P. F. Glas, "Digital I/Q imbalance compensation in a low-IF receiver," in *Proc. IEEE Globecom 98*, Sydney, Australia, Nov. 1998, pp. 1461-1466.

[8] L. Yu and W. M. Snelgrove, "A novel adaptive mismatch cancellation system for quadrature IF radio receivers," *IEEE Trans. Circuits Syst. II*, vol. 46, pp. 789-801, Jun. 1999.

[9] T. Hentschel and G. Fettweis, "Software radio receivers," Chapter 10 in *CDMA Techniques for Third Generation Mobile Systems*, edited by F. Swarts, P. van Rooyan, I. Oppermann, and M. P. Lötter. Boston, MA: Kluwer Academic Publishers, 1999.

[10] E. A. Lee and D. G. Messerschmitt, *Digital Communication*. Boston, MA: Kluwer Academic Publishers, 1988.

[11] S. Haykin, *Adaptive Filter Theory*, 3rd ed. Upper Saddle River, NJ: Prentice-Hall, 1996.

[12] S. Haykin, ed., *Unsupervised Adaptive Filtering, vol I: Blind Source Separation*. New York: John Wiley & Sons, 2000.

[13] S. Amari, S. C. Douglas, A. Cichocki, and H. H. Yang, "Multichannel blind deconvolution and equalization using the natural gradient," *in Proc. IEEE Workshop on Signal Processing Advances in Wireless Communications*, Paris, France, Apr. 1997, pp. 101-104.